

# Effect of Shot Peening and Plasma Electrolytic Oxidation on the Intergranular Corrosion Behavior of 7A85 Aluminum Alloy

Zuoyan Ye · Daoxin Liu · Chongyang Li · Xiaoming Zhang · Zhi Yang · Mingxia Lei

Received: 17 November 2013 / Revised: 30 December 2013 / Published online: 26 July 2014  
© The Chinese Society for Metals and Springer-Verlag Berlin Heidelberg 2014

**Abstract** The effects of shot peening (SP) and plasma electrolytic oxidation (PEO) on the intergranular corrosion behavior of the novel high strength aluminum alloy 7A85 (AA 7A85) were investigated by electrochemical polarization and electrochemical impedance tests. The intergranular corrosion mechanism of SP, PEO and PEO combined with sealing-treated AA 7A85 was studied by the metallographic analysis, residual stress testing, X-ray diffractometer analysis and scanning electron microscopy. The results show that AA 7A85-T7452 is very sensitive to intergranular corrosion. SP would significantly improve its intergranular corrosion resistance. This is attributed to the combination action of residual compressive stress and grain refinement. PEO would reduce the largest corrosion depth by 41.6%. Moreover, PEO without sealing did not eliminate the intergranular corrosion due to the existence of the micropores and microcracks in the oxide coating. However, PEO combined with the SiO<sub>2</sub> sol–gel sealing treatment could effectively protect the AA 7A85-T7452 from intergranular corrosion because of the good corrosion resistance and barrier function of the sealed coating.

**KEY WORDS:** 7A85 aluminum alloy; Plasma electrolytic oxidation; Shot peening; Intergranular corrosion; Residual stress

## 1 Introduction

Aluminum alloy 7085 (AA7085) had been developed in 2003 by Alcoa as the next generation of high strength, high toughness and low quenching sensitivity alloy for an urgent need of thick aluminum forgings for the next generation aircraft. It has been successfully applied to large aircraft such as Boeing 787 for main bearing components [1]. Drawing on the advanced characteristics of this material, China developed 7A85 aluminum alloy, its performance

can be comparable with AA7085, and laid a good material foundation for the development of new advanced aircraft. Comparing with other 7xxx aluminum alloy, AA7085 has high fracture toughness and low quench sensitivity due to the higher zinc along with the lower copper content. Generally, the combination of high strength and good corrosion resistance was contradictory. For example, higher Zn content increased the strength while decreased the corrosion resistance. The T6 peak age temper provided high strength, but low corrosion resistance. The T7x over-aged temper increased the corrosion resistance, but sacrificed some strength. In order to achieve both high strength and good corrosion resistance, lots of effort have been carried out on the developing of new heat treatment process. For example, retrogression and reaging (RRA) temper increased the corrosion resistance while kept the strength levels similar to T6 temper [2]. Two-step aging temper gained higher stress corrosion cracking resistance and strength than that of T6 temper [3]. However, the effects of

Available online at <http://link.springer.com/journal/40195>

Z. Ye · D. Liu (✉) · C. Li  
Corrosion and Protection Research Laboratory, Northwestern  
Polytechnical University, Xi'an 710072, China  
e-mail: Liudaox@nwpu.edu.cn

X. Zhang · Z. Yang · M. Lei  
AVIC the First Aircraft Institute, Xi'an 710089, China

temper on strength and corrosion resistance of Al alloys with different compositions differed greatly [4]. So it is difficult to achieve a good combination performance of new Al alloys by the current heat treatment process.

Surface treatment technology can obtain the desired surface performance without changing the overall property of materials. Numerous surface treatment technologies have been applied to aluminum alloys, such as anodic oxidation, plasma electrolytic oxidation (PEO), shot peening (SP), nitriding, electroplating, and vacuum coating, in which SP and anodic oxidation are widely used in the aerospace industry. SP was mainly used to improve the fatigue and stress corrosion cracking resistance of aircraft aluminum alloy [5, 6], while studies on the influence of SP on the corrosion resistance are less reported [7]. PEO could produce ceramic coatings on the aluminum alloy surface in situ. The coating thickness, hardness and density are significantly improved compared with conventional anodic oxide film. In recent years, much attention has been attracted to the PEO technology for its good prospects in the aviation industry. The effect of PEO on the uniform corrosion of aluminum alloy has been widely investigated [7, 8], but for the intergranular corrosion (IGC) of new high strength, aluminum alloy applied in the aircraft structure in acid environment is less reported. However, aircraft structure would be frequently under the aggressive environment such as acid rain or occluded area. So localized corrosion such as the intergranular corrosion and exfoliation corrosion is easily occurred. As mentioned above, the effect of SP and PEO on the corrosion behavior of novel high strength 7A85 aluminum alloy in acid IGC solution was studied. The purpose of this article was to provide a reference for improving IGC performance of new aluminum alloy 7A85 using these two surface treatment technologies on.

## 2 Experimental

### 2.1 Materials and Specimens

The present investigation was carried out on the 220-mm-thick 7A85 aluminum alloy plate with chemical composition of (wt%): Zn 7.76, Mg 1.69, Cu 1.75, Fe 0.026, Si 0.013, Zr 0.017, Ti 0.0022, and remainder Al balanced. The plates were solution treated at 470 °C for 1 h, quenched in room temperature water, compressed to generate a 1–5% constant deformation and then aged at 110 °C for 6 h and 160 °C for 10 h. All the specimens were sampled at the surface of the forging by machinery cutting. Samples for IGC tests and electrochemical tests were flat rectangular specimens with dimensions of 40 mm × 25 mm × 5 mm and 15 mm × 15 mm × 5 mm, respectively. The through-

thickness direction of samples was the same as that of the forging.

### 2.2 Surface Treatments

Specimens were firstly polished to 1200# emery paper, then cleaned in anhydrous alcohol and distilled water. Test specimens were prepared with four different surface finishes: polishing, SP, PEO and PEO combined with sealing (PEO + S) treatment. SP specimens were shot peened by glass shots with 100% surface coverage and 0.15 mm Almen intensity. PEO treatment was performed in an alkaline silicate solution (NaOH 1 g/L, Na<sub>2</sub>SiO<sub>3</sub> 15 g/L) with additions of (NaPO<sub>3</sub>)<sub>6</sub> 10 g/L and NaAlO<sub>2</sub> 1 g/L. A pulsed bipolar current supply was used with frequency set at 1 kHz and current ≈ 0.6 mA/cm<sup>2</sup>. The temperature of the electrolyte was maintained at (20 ± 2) °C using a heat exchanger throughout the coating process. Samples were treated for 1 h then took out of the electrolyte, thoroughly washed in cold running water, ultrasonically cleaned in the anhydrous alcohol and dried. The average thickness of the PEO coating was 35 μm.

The sol used for sealing consisted of TEOS, ethanol and distilled water (the volume ratio is 2:4:1), and the pH value of the sol was adjusted to be 3–4 by diluted hydrochloric acid. The size of SiO<sub>2</sub> particles obtained by hydrolysis of the TEOS in an acidic environment was in nanometer scale. In the sealing process, PEO-treated samples were immersed in the sol after cleaning, ultrasonic vibration for 1 min to exhaust the air in the coating defects. Negative pressure was formed in the defects, and the sol particles were inhaled. Then removed the sample from the sol vertically, the sample surface will be covered with a sol layer, after solidifying at room temperature for 24 h and baking at 120 °C for 1 h, a SiO<sub>2</sub> gel layer formed on the surface of PEO coating.

### 2.3 Corrosion Test

The corrosion resistance of the base material (BM) and surface-treated specimens was examined by intergranular corrosion (IGC) solution immersion tests. A liter intergranular corrosion solution contained 30 g NaCl and 10 mL HCl (36 wt%). The ratio of specimen area to solution volume is <200 cm<sup>2</sup>/L. The IGC immersion test was carried out at 35 °C for 24 h. After IGC test, samples were immersed in dilute nitric acid to remove the corrosion products, then rinsed thoroughly with running water and dried in air. The surface corrosion morphology was recorded by photographing. A 5-mm-long part was cut out from the bottom of the sample and mounted with bakelite. The mounted samples were polished to measure the corrosion depth by optical microscopy.

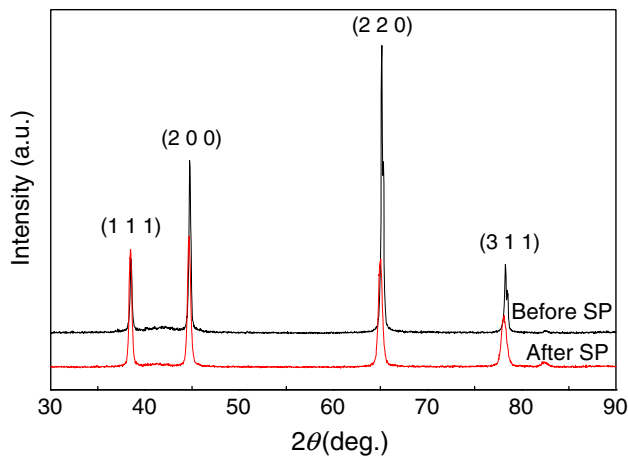


**Fig. 1** XRD patterns of 7A85 alloy before and after SP

## 2.4 Characterization

The surface morphology after corrosion was recorded by a camera. The roughnesses of the polished and shot peened samples were measured by SurfTest SJ201 roughmeter. The residual stress of the shot peened samples was determined by D/MAX 2200 PC X-ray stress analyzer. The morphology and composition of PEO coating were analyzed using a JEOL JSM-6360LV SEM with EDS. Coating phase analysis was investigated using a Siemens D5000 X-ray diffractometer (XRD) in a standard  $2\theta$  arrangement between  $10^\circ$  and  $90^\circ$ . The coating thickness and the corrosion depth measurements were performed by optical microscopy equipped with a digital camera. Electrochemical studies were conducted in IGC solution using a PARSTAT-2273 Electrochemical workstation. A standard three-electrode system with the sample as the working electrode, a saturated calomel electrode (SCE) as the reference electrode and a platinum sheet as the counter electrode, was used in the tests. Measurements were taken in IGC solution, and the exposed area was  $1\text{ cm}^2$ . Equivalent circuits were modeled using ZView software.

## 3 Results

### 3.1 Influence of SP on Alloy Surface Integrity

Surface integrity changes induced by shot peening mainly include three parts [9]: increasing surface roughness, refining surface layer grains and introducing a certain depth residual compressive stress. The surface roughness of polished base material samples was  $R_a = 0.08\ \mu\text{m}$ . After shot peening, the roughness is increased to  $R_a = 2.07\ \mu\text{m}$ . Figure 1 shows the XRD patterns of polished surface and shot peened surface. The broadening of diffraction peak

indicated that shot peening refined the surface grains. The shifting of the peak location of SP sample was induced by the residual stress. The residual stress of shot peened sample surface was measured to be  $-149\text{ MPa}$ , but that of the polished base material was about  $0\text{ MPa}$ .

### 3.2 Characterization of PEO and PEO + S Coating

Figure 2a shows the SEM image of PEO coating surface. From the SEM image, it can be seen that many micropores and microcracks existed on the coating surface. Micropores were formed by molten salts and gas bubbles thrown out of microarc discharge channels. Microcracks were induced by thermal stress due to rapid solidification of molten oxide in the cool electrolyte. The existence of pores and cracks decreased the corrosion resistance of the oxide coating.  $\text{SiO}_2$  sol-gel treatment was employed to seal the PEO coating. Figure 2b shows the SEM image of sealed coating surface. After sealing treatment, micropores and cracks were filled and the coating surface was smoothed.

Figure 3a shows the cross-sectional SEM image of the PEO coating. The oxide coating was closely combined with the aluminum alloy substrate. Micropores and microcracks also can be seen in the cross-sectional view of the coating, and microcracks were mainly distributed in the outer layer of the coating.

Energy dispersive spectrometer (EDS) and X-ray diffraction (XRD) were used to analysis the chemical composition and phase of PEO coating, and the results are shown in Fig. 3b. As it can be seen, qualitatively, the chemical composition of the coating is mainly Al, O and Si. This indicated that the PEO coating was mainly composed of aluminum oxide. The XRD spectra indicated that the oxide coating was mainly composed of  $\alpha\text{-Al}_2\text{O}_3$  and  $\gamma\text{-Al}_2\text{O}_3$ . The Al phase was from substrate. The oxide coating can be divided into two parts: a porous outer layer and a more compact inner layer. The inner layer mainly was composed of  $\alpha\text{-Al}_2\text{O}_3$ , but the outer layer mainly was composed of  $\gamma\text{-Al}_2\text{O}_3$ . Silicon mainly existed in the  $\text{SiO}_2$  and the  $\text{Al}_2\text{SiO}_5$  phase of the oxide coating [10].

### 3.3 Electrochemical Behavior of PEO and PEO + S Coating

Potentiodynamic polarization and electrochemical impedance spectroscopy were used to evaluate the corrosion resistance of the samples with different surface finishes.

The polarization curves are shown in Fig. 4. Corrosion potential ( $E_{\text{corr}}$ ), corrosion current density ( $I_{\text{corr}}$ ) and polarization resistance ( $R_p$ ) values are presented in Table 1. Compared to that of the base material, the  $E_{\text{corr}}$  and  $I_{\text{corr}}$  of SP sample are increased slightly. The positive shift of  $E_{\text{corr}}$

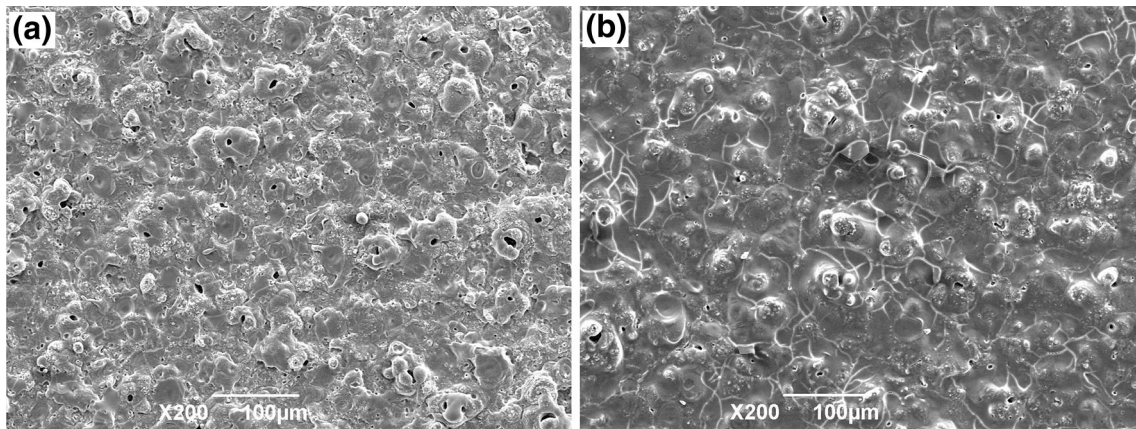


**Fig. 2** Surface morphology of coatings: **a** PEO; **b** PEO + S

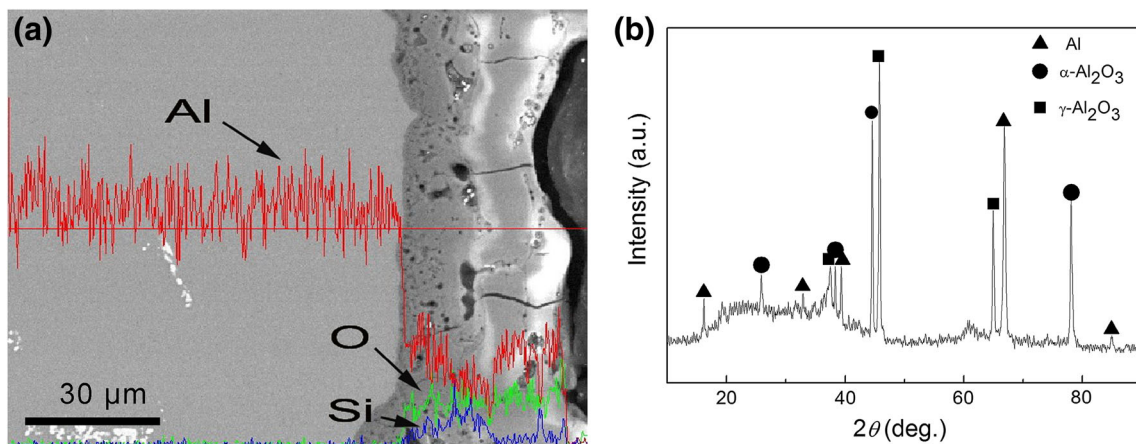


**Fig. 3** Cross-sectional element distribution **a** & XRD pattern **b** of PEO coating surface

**Table 1** Calculated Tafel parameters from the polarization plots

Surface	$E_{\text{corr}}$ (V)	$I_{\text{corr}}$ (A/cm <sup>2</sup> )	$R_p$ (Ω/cm <sup>2</sup> )
BM	-0.765	$1.20 \times 10^{-3}$	$8.17 \times 10^3$
SP	-0.758	$3.26 \times 10^{-3}$	$5.78 \times 10^3$
PEO	-0.749	$1.22 \times 10^{-4}$	$1.32 \times 10^5$
PEO + S	-0.740	$2.28 \times 10^{-7}$	$8.09 \times 10^7$

is due to the residual compressive stress [11], and the increasing of  $I_{\text{corr}}$  is attributed to the enlarging of the real exposure area induced by shot peening. Although the initial current density of SP sample at free corrosion status is raised, but after the rough surface is etched off (at anodic polarization condition), the current density becomes lower than that of the BM sample. Sealing treatment had no significant effect on the  $E_{\text{corr}}$  of PEO coating, but decreased the  $I_{\text{corr}}$  by three orders of magnitude. As an insulating material, the SiO<sub>2</sub> sol-gel sealant did not change the  $E_{\text{corr}}$ . While sealing treatment filled the micropores and

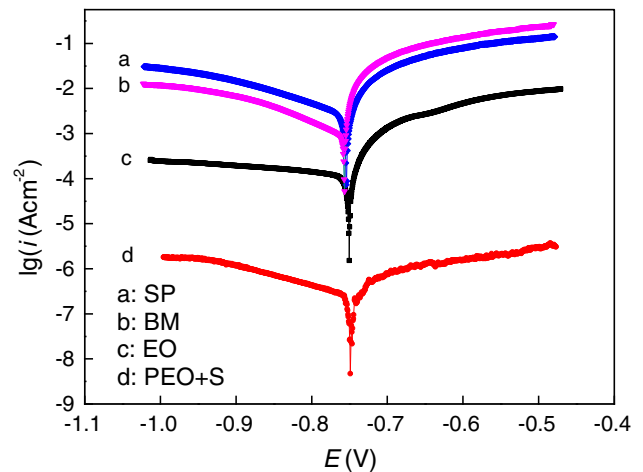


**Fig. 4** Tafel polarization plots for samples with different surface finishes after immersion in IGC solution at 35 °C for 30 min

microcracks so that isolated the base material from the corrosive solution, the corrosion current is significantly reduced (Fig. 4).

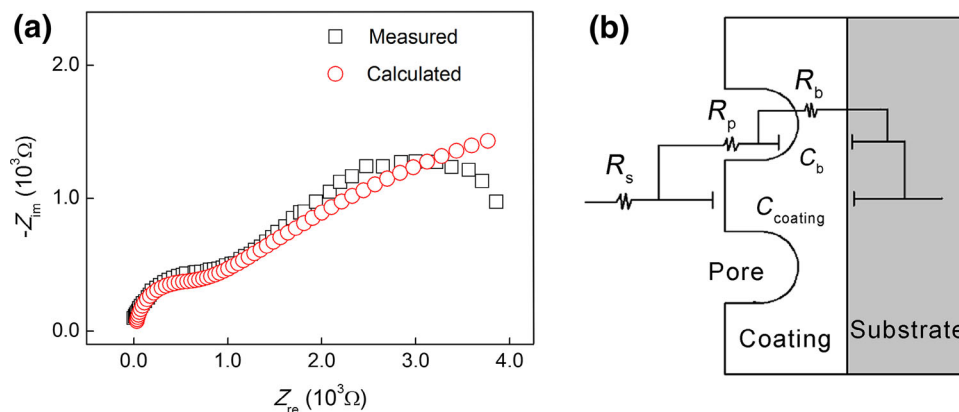


**Fig. 5** Electrochemical impedance spectrum **a** & equivalent circuit **b** for PEO coating after immersion in IGC solution at 35 °C for 10 min

Figure 5a shows the Nyquist impedance plots of PEO coating after immersion in IGC solution for 10 min. The EIS equivalent circuit for aluminum electrode with porous alumina coatings is proposed in Fig. 5b [10, 12], and the calculated parameters are shown in Table 2. As seen from the equivalent circuit, the impedance of the measured system between reference electrode and working electrode was consisted of 3 parts: the electrolyte, the outer porous layer and the inner compact layer.  $R_s$  is the electrolyte resistance,  $R_p$  is the resistance of the outer porous layer,  $C_{\text{coating}}$  is the capacitance of the whole PEO coating,  $R_b$  and  $C_b$  are the inner barrier layer resistance and capacitance, respectively. The Nyquist impedance plots and EIS equivalent circuit of the PEO + S coating are shown in Fig. 6. After sealing treatment, the pores and cracks were filled and the surface of the oxide coating was covered by a thin layer of  $\text{SiO}_2$  gel. Sealing treatment changed the structure of PEO coating and made the coating to be a compact barrier. The EIS equivalent circuit for sealed coating is proposed in Fig. 6b [13].  $R_s$  is the electrolyte resistance,  $R_{\text{coating}}$  is the coating resistance, and  $C_{\text{coating}}$  is the capacitance of sealed coating. The calculated parameters are shown in Table 2. From the EIS curves, it can be seen that the electric resistance of PEO coating increased by two orders of magnitude after sealing, so sealing plays an important role in improving the corrosion resistance of PEO coating.

#### 3.4 Effect of Surface Treatments on the IGC Performance

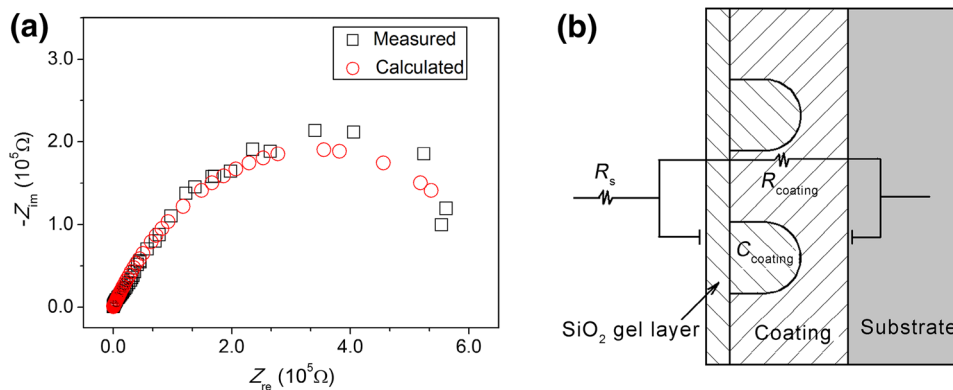
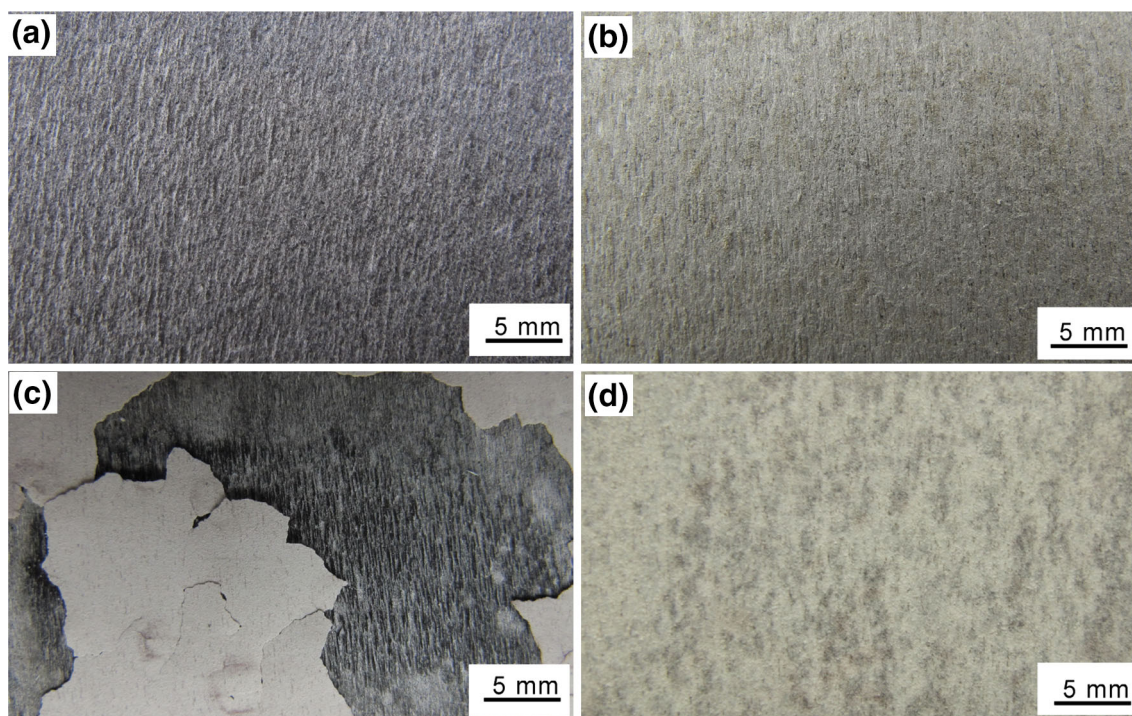
When immersed in IGC solution, the BM and SP samples reacted quickly with the solution, a large number of bubbles were produced at the surface of samples. SP treatment increased the effective surface area of samples, so the real contact area of SP sample with the IGC solution is larger than that of polished one. Gas evolution on SP samples was

much more intensive than that on polished samples. No corrosion reaction was observed on the surface of PEO and PEO + S samples at the beginning of immersion. After immersed for 1 h, the polished 7A85 base material and SP samples had lost metallic luster and the number of bubbles decreased. A few bubbles began to form on the PEO coating surface, with extension of the immersion time, the number of pores giving off gas is increasing. Then, the coating surface began to blister and the PEO coating flaked off with the bursting of blisters. No corrosion was observed on the PEO + S-treated samples after immersion in IGC solution for 24 h. Even extending the immersion time to 100 h, the composite-treated samples were also not corroded. Figure 7 shows the surface morphologies of samples after immersion in IGC solution for 24 h. As can be seen, the surface roughness of polished samples was significantly increased due to the appearance of ridges along the rolling direction. The ridges also appeared on the surface of SP samples, but they were shorter than that on the polished samples. Almost, all of the coating of PEO samples was flaked off after the corrosion test and the corrosion morphology of the exposed base material was the same with that of the polished samples. The immersion only induced light discoloration on the PEO + S composite-treated samples, and the coating remained intact after the corrosion test.

Figure 8 shows the cross-sectional morphologies of samples with different surface finishes after corrosion tests. The grain boundaries network of BM samples can be seen clearly, and corrosion affected a deep zone. The corrosion depth of SP samples is less than that of BM sample, but intergranular corrosion also occurred (Fig. 8b). After IGC immersion test, most of the coating of PEO sample was flaked off and the corrosion morphology of exposed area is the same as that of the BM sample (Fig. 8c). The corrosive solution had penetrated the PEO coating and induced serious intergranular corrosion to base material. However,

**Table 2** Calculated impedance parameters of PEO and PEO + S coatings

Coating	$R_s$ ( $\Omega/\text{cm}^{-2}$ )	$R_p$ ( $\Omega/\text{cm}^{-2}$ )	$C_{\text{coating}}$ ( $\text{F}/\text{cm}^2$ )	$R_b$ ( $\Omega/\text{cm}^{-2}$ )	$R_{\text{coating}}$ ( $\Omega/\text{cm}^{-2}$ )	$Q(C_b)$ ( $\Omega^{-1}/\text{cm}^2/\text{s}^{-n}$ )	$Q - n$
PEO	18.9	411.5	$1.904 \times 10^{-8}$	$6.142 \times 10^3$	–	$3.479 \times 10^{-5}$	0.46
PEO + S	19.8	–	$2.460 \times 10^{-7}$	–	$6.851 \times 10^5$	–	–

**Fig. 6** Electrochemical impedance spectrum **a** & equivalent circuit **b** for PEO + S coating after immersion in IGC solution at 35 °C for 10 min**Fig. 7** Corrosion morphologies of different samples after 24-h immersion: **a** BM; **b** SP; **c** PEO; **d** PEO + S

there is no corrosion on the PEO + S sample for the good corrosion resistance of the sealed coating (Fig. 8d).

The corrosion depths of different samples are shown in Table 3. The 7A85 aluminum alloy base material sample suffered serious intergranular corrosion, and the most corrosion depth reaches 200  $\mu\text{m}$ . Shot peening treatment significantly decreased the IGC sensitivity of 7A85

aluminum alloy, and the corrosion depth of SP sample is less than half of that of BM samples. The PEO coating delayed the contacting between IGC solution and the base material, so decreased the corrosion sensitivity in a certain extent. The barrier layer formed by PEO and sealing composite treatment isolated the corrosion environment from the base material, so the base material was protected

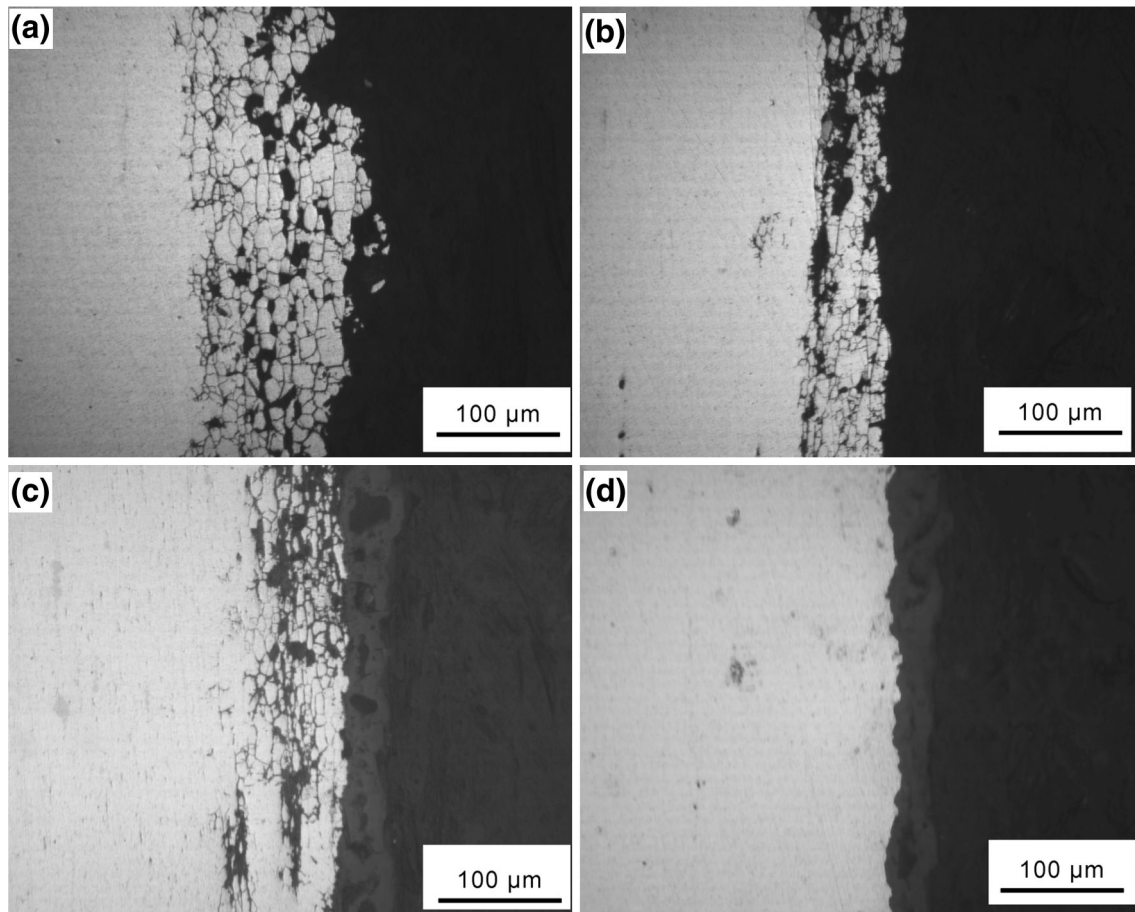


**Fig. 8** Cross-sectional morphologies of different samples after IGC tests: **a** BM; **b** SP; **c** PEO; **d** PEO + S

**Table 3** Intergranular corrosion depth of samples with different surface finishes

Surface states	Average depth ( $\mu\text{m}$ )	Maximum depth ( $\mu\text{m}$ )
BM	176.4	200.2
SP	61.5	77.4
PEO	108.7	116.9
PEO + S	0	0

against corrosion. Corrosion sensitivity can be evaluated by the corrosion depth, and the ranking from low to high in order is as follows: PEO + S samples, SP samples, PEO samples and BM samples.

## 4 Discussion

### 4.1 Effect of SP Treatment on the IGC Performance of 7A85 Al Alloy

The mechanical property and corrosion performance of high strength aluminum alloy mainly depend on the microstructure

such as matrix precipitates (MPt), grain boundary precipitates (GBP) and precipitation free zone (PFZ). GBP and PFZ play an important role in the IGC behavior of aluminum alloy. Although the effect mechanism of GBP and PFZ is not fully understood, but it has been widely accepted that the decreasing of copper content or increasing of zinc content in the GBP could result in the increasing of corrosion sensitivity of aluminum alloy [14]. Intergranular corrosion initials at the alloy surface and extends to inner material along the grain boundaries. GBP generally corroded firstly as the anode. If GBP distributes continuously, the dissolution of GBP forms corrosion tunnel. The corrosion products have a larger volume than the original material and the expansion causes stresses that lift the grains, so the corrosion continually extends to the inner base material [15].

7A85 aluminum alloy has a large grain size, so the proportion of the grain interior to the grain boundary is considerable high. When the alloy suffered corrosion, the grain interior acted as the cathode and the grain boundary acted as the anode. This “big cathode-little anode” structure would promote the development of corrosion. SP refined the surface grains of 7A85 alloy, and the proportion of the grain

interior to the grain boundary was reduced. The microstructure of aluminum alloy became more uniform, so the localized corrosion was inhibited and the corrosion tended to be homogenized. The refinement of grains destructed the continuous distribution of GBP, while prevented the formation of anode corrosion tunnel and inhibited the intergranular corrosion from extending to the inner material. SP also could introduce residual compressive stress to the alloy surface. The compressive stress normal to the grain boundaries significantly reduced the number of active sites [16] and counteracted part of the expansion stress introduced by corrosion products, so the initialing and developing of intergranular corrosion was retarded. SP increased the alloy surface roughness, so the real contact area of samples and solution was raised, and the uniform corrosion rate was promoted. But beneficial factor can be dominated by choosing proper shot peening parameters, and reasonable shot peening can effectively enhance the intergranular corrosion resistance of 7A85 aluminum alloy.

#### 4.2 Effect of Sealing on the Electrochemical Behavior of PEO Coating

As shown in Table 1, the sealing treatment had no significant effect on the  $E_{\text{corr}}$  of the PEO coating, but increased the  $R_p$  by almost three orders of magnitude and decreased the  $I_{\text{corr}}$  by three orders of magnitude. This is because there are many micropores and microcracks in the unsealed coating, so corrosive ions could reach the base material through these defects and reacted with the aluminum alloy. The electronic exchanging induced large corrosion current. After sealing treatment, the PEO coating became integrated and compact. The PEO + S coating could effectively protect the aluminum alloy from corrosion, and the corrosion current was remarkably decreased.

As can be known from Table 2, the inner compact layer of the PEO coating has much higher corrosion resistance than the outer porous layer, the corrosion resistance of the whole PEO coating would mostly be determined by the inner compact layer [11]. The  $\text{SiO}_2$  sol–gel sealing treatment filled the pores and cracks of the PEO coating and formed a  $\text{SiO}_2$  gel layer on the surface of coating. It is reasonable that different equivalent circuits were used to analysis the electrochemical impedance spectra of sealed and unsealed PEO coating. The whole electric resistance of PEO coating increased by two orders of magnitude with sealing, so the protection of the PEO coating was significantly enhanced.

#### 4.3 Effect of PEO and PEO + S on the IGC Behavior of 7A85 Aluminum Alloy

The oxide coating is mainly composed of  $\alpha$ -alumina (the inner compact layer) and  $\gamma$ - $\text{Al}_2\text{O}_3$  (the outer porous layer).

The nucleation energy of  $\gamma$ - $\text{Al}_2\text{O}_3$  is less than  $\alpha$ -alumina, so the melting matter ejected from the discharge channel rapidly solidified at the electrolyte interface which favored the formation of  $\gamma$ - $\text{Al}_2\text{O}_3$  outside.  $\alpha$ - $\text{Al}_2\text{O}_3$  is a high temperature stable phase, while  $\gamma$ - $\text{Al}_2\text{O}_3$  is a low temperature stable phase. The coating temperature increased with the plasma discharge processing, and some  $\alpha$ - $\text{Al}_2\text{O}_3$  would transform to  $\gamma$ - $\text{Al}_2\text{O}_3$ .

As shown in Figs. 2 and 3, many micropores and microcracks exist in the PEO coating. Micropores were formed by residual gas evolution channels during microarc process, and microcracks were generated due to thermal stress during rapid solidification of molten oxide in the cool electrolyte. So the PEO coating has a lot of defects. When the coating is in corrosive environment, corrosive medium will reach the aluminum alloy substrate along these defects, resulting in corrosion of the substrate. After reached the substrate, corrosive ions penetrated to the inner aluminum alloy along the grain boundaries and caused intergranular corrosion of the substrate. Meanwhile, corrosive ions penetrated along the interface of PEO coating and aluminum alloy substrate, corroded the interface and formed crevice corrosion. PEO coating ruptured then flaked off with the effect of bubbles produced by corrosion of aluminum alloy substrate. PEO coating lost its protection function, and aluminum alloy substrate was exposed to the corrosive solution. However, PEO coating can delay the corrosive ions reaching the substrate. Within 1-h immersion, no corrosion was observed on PEO samples, while with immersion time increasing, corrosive ions reached the substrate through the defects of coating and reacted with the aluminum alloy substrate. Bubbles began to emerge from some pores on the coating surface. The number of bubbles and pores producing bubbles increased with extension of immersion time. PEO coating without sealing treatment cannot effectively protect the aluminum alloy substrate from the intergranular corrosion while reduced the corrosion in a certain extent by delaying the contact of corrosive medium and aluminum alloy substrate.

After  $\text{SiO}_2$  sol–gel sealing treatment, the most micropores disappeared and microcracks also were closed (Fig. 2b).  $\text{SiO}_2$  gel layer itself has strong corrosion resistance, so the  $\text{SiO}_2$  sol–gel sealed PEO coating can effectively protect the aluminum alloy substrate from the intergranular corrosion by insulating corrosive medium.

## 5 Conclusions

1. 7A85-T7452 aluminum alloy is sensitive to the intergranular corrosion. Severe intergranular corrosion occurred during immersing in IGC solution for 24 h.
2. Shot peening could decrease the intergranular corrosion sensitivity of 7A85-T7452 aluminum alloy

obviously for the combined action of the residual compressive stress and grain refinement, but could not eliminate the intergranular corrosion.

3. PEO could not effectively protect the aluminum alloy substrate for the existing of micropores and microcracks. The SiO<sub>2</sub> sol–gel sealing treatment could fill the micropores and microcracks of the PEO coating and produce a SiO<sub>2</sub> gel layer on the coating surface. The sealed PEO coating can eliminate intergranular corrosion of 7A85-T7452 aluminum alloy by insulating the corrosive medium from the substrate.

**Acknowledgments** This work was financially supported by the National Natural Science Foundation of China (No. 51171154).

## References

- [1] D.J. Chakrabarti, J. Liu, R.R. Sawtell, G.B. Venema, Mater. Forum **28**, 969 (2004)
- [2] M.C. Baruch, U.S. Patent 3856584 (1974)
- [3] D. Wang, D.R. Ni, Z.Y. Ma, Mater. Sci. Eng. A **494**, 360 (2008)
- [4] S.Y. Chen, K.H. Chen, G.S. Peng, L. Jia, P.X. Dong, Mater. Des. **35**, 93 (2012)
- [5] S. Curtis, E.R. de Los Rios, C.A. Rodopoulos, A. Levers, Int. J. Fatigue **25**, 59 (2003)
- [6] D.T. Asquith, A.L. Yerokhin, J.R. Yates, A. Matthews, Thin Solid Films **515**, 1187 (2006)
- [7] D.T. Asquith, A.L. Yerokhin, J.R. Yates, A. Matthews, Thin Solid Films **516**, 417 (2007)
- [8] T.B. Wei, F.Y. Yan, J. Tian, J. Alloys Compd. **389**, 169 (2005)
- [9] X.H. Zhang, D.X. Liu, Int. J. Fatigue **31**, 889 (2009)
- [10] V. Raj, M. Mubarak Ali, J. Mater. Process. Technol. **209**, 5341 (2009)
- [11] J.H. Liu, D. Li, P.Y. Liu, B.L. Lan, J. Mater. Eng. (2), 30 (2005) (in Chinese)
- [12] A. Venugopal, R. Panda, S. Manwatkar, K. Sreekumar, L.R. Krishna, G. Sundararajan, Trans. Nonferr. Met. Soc. **22**, 700 (2012)
- [13] X.W. Yu, C.N. Cao, Thin Solid Films **423**, 252 (2003)
- [14] J. Wloka, T. Hack, S. Virtanen, Corros. Sci. **49**, 1437 (2007)
- [15] D. McNaughtan, M. Worsfold, M.J. Robinson, Corros. Sci. **45**, 2377 (2003)
- [16] X.D. Liu, G.S. Frankel, Corros. Sci. **48**, 3309 (2006)